BIOCHEMISTRY
including biophysical chemistry & molecular biology
Article

Biochemistry **2011,** *50,* 1265–1273 1265
DOI: 10.1021/bi101794y

Proline 96 of the Copper Ligand Loop of Amicyanin Regulates Electron Transfer from Methylamine Dehydrogenase by Positioning Other Residues at the Protein−Protein Interface[†,‡]

Moonsung Choi,[§] Narayanasami Sukumar,[∥] F. Scott Mathews,[⊥] Aimin Liu,[#] and Victor L. Davidson*[,§]

[§]*Department of Biochemistry, University of Mississippi Medical Center, Jackson, Mississippi 39216, United States,* [∥]*NE-CAT and Department of Chemistry and Chemical Biology, Cornell University, Building 436E, Argonne National Laboratory, Argonne, Illinois 60439, United States,* [⊥]*Department of Biochemistry and Molecular Biophysics, Washington University School of Medicine, St. Louis, Missouri 63110, United States, and* [#]*Department of Chemistry, Georgia State University, Atlanta, Georgia 30302, United States*

Received November 9, 2010; Revised Manuscript Received December 30, 2010

ABSTRACT: Amicyanin is a type 1 copper protein that serves as an electron acceptor for methylamine dehydrogenase (MADH). The site of interaction with MADH is a "hydrophobic patch" of amino acid residues including those that comprise a "ligand loop" that provides three of the four copper ligands. Three prolines are present in this region. Pro94 of the ligand loop was previously shown to strongly influence the redox potential of amicyanin but not affinity for MADH or mechanism of electron transfer (ET). In this study Pro96 of the ligand loop was mutated. P96A and P96G mutations did not affect the spectroscopic or redox properties of amicyanin but increased the K_d for complex formation with MADH and altered the kinetic mechanism for the interprotein ET reaction. Values of reorganization energy (λ) and electronic coupling (H_{AB}) for the ET reaction with MADH were both increased by the mutation, indicating that the true ET reaction observed with native amicyanin was now gated by or coupled to a reconfiguration of the proteins within the complex. The crystal structure of P96G amicyanin was very similar to that of native amicyanin, but notably, in addition to the change in Pro96, the side chains of residues Phe97 and Arg99 were oriented differently. These two residues were previously shown to make contacts with MADH that were important for stabilizing the amicyanin−MADH complex. The values of K_d, λ, and H_{AB} for the reactions of the Pro96 mutants with MADH are remarkably similar to those obtained previously for P52G amicyanin. Mutation of this proline, also in the hydrophobic patch, caused reorientation of the side chain of Met51, another reside that interacted with MADH and caused a change in the kinetic mechanism of ET from MADH. These results show that proline residues near the copper site play key roles in positioning other amino acid residues at the amicyanin−MADH interface not only for specific binding to the redox protein partner but also to optimize the orientation of proteins for interprotein ET.

Transition metals are used in proteins as structural elements and components of catalytic and redox-active centers (*1*). Several proteins contain copper which participates in a variety of biological functions ranging from activation of dioxygen to mediation of electron transfer (ET).[1] Copper sites in proteins have been classified according to their spectroscopic and functional properties as type 1, type 2, or type 3 (*2*). A type 1, or blue copper, site is so named for an intense absorption band near 600 nm ($\varepsilon \sim 5000$ M^{-1} cm^{-1}) attributable to a cysteine S to Cu(II) charge transfer (*3*). Blue copper sites function as efficient ET mediators, and their oxidation−reduction midpoint potential (E_m) values span a wide range from +200 to +1000 mV (*4*). Amicyanin (*5*) is a type 1 copper protein that is involved in metabolism of methylamine by several methylotrophic and autotrophic bacteria. In *Paracoccus denitrificans*, amicyanin mediates ET from methylamine dehydrogenase (MADH) (*6*) to cytochrome c_{551i} (*7*), and these electrons are ultimately donated to the membrane-bound respiratory chain. A crystal structure of the complex of MADH, amicyanin, and cytochrome c_{551i} has been determined (*8*), and in the crystalline state the complex is catalytically active (*9*, *10*) and transfers electrons from the tryptophan tryptophylquinone (TTQ) (*11*) cofactor of MADH to the cytochrome heme via the copper site of amicyanin. While MADH, amicyanin, and cytochrome c_{551i} are isolated as individual soluble proteins, it has been demonstrated that in solution they must form a ternary complex to catalyze methylamine-dependent cytochrome c_{551i} reduction (*12*, *13*). The ET reactions to (*14*−*17*) and from (*18*) the type 1 copper center of amicyanin within the protein complex have been studied in solution by stopped-flow spectroscopy. Analysis by ET theory (*19*) of the temperature dependencies of

[†]This work was supported by NIH Grant GM-41574 (V.L.D.) and NSF Grant MCB 0843537 (A.L.). This work and the 24ID-C beamline used to collect data were supported by RR-15301 (NE-CAT facility at the APS) from NCRR of NIH. Use of the APS is supported by the U.S. DOE, Office of Science, Office of Basic Energy Science, Contract No. DE-AC02-06CH11357.

[‡]Crystallographic coordinates have been deposited in the Protein Data Bank under the file name 3PLY for Cu(II) P96G amicyanin.

*Address correspondence to this author. Tel: 601-984-1516. Fax: 601-984-1501. E-mail: vdavidson@umc.edu.

[1]Abbreviations: MADH, methylamine dehydrogenase; TTQ, tryptophan tryptophylquinone; ET, electron transfer; E_m, oxidation−reduction midpoint potential; H_{AB}, electronic coupling; λ, reorganization energy; rms, root mean square.

Published on Web 01/10/2011

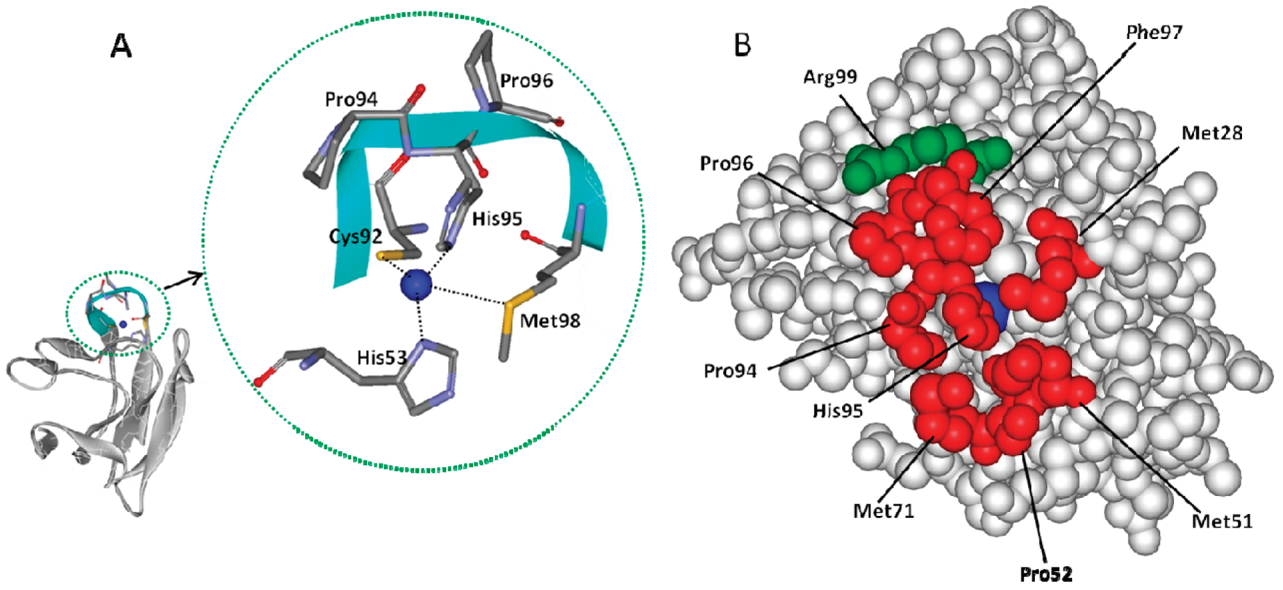

FIGURE 1: The structure of native amicyanin. (A) The secondary structure of amicyanin is shown with the ligand loop highlighted in light blue and enlarged in the circle. (B) A space-filling model of amicyanin with the residues that comprise the hydrophobic patch indicated in red and Arg99 which forms a salt bridge with MADH colored green. Copper is shown as a blue sphere.

Table 1: Comparison of Sequences of the C-Terminal Ligand-Containing Loops of the Major Classes of Cupredoxins

Protein	Ligand-containing C-terminal loops[a]
Amicyanin[b]	**C** T **P** **H** **P** F **M**
Azurin[c]	**C** T F **P** G **H** S A L **M**
Pseudoazurin[d]	**C** T **P** **H** Y A M G **M**
Plastocyanin[e]	**C** S **P** **H** Q G A G **M**
Stellacyanin[f]	**C** G V **P** K **H** C D L G **Q**
Rusticyanin[g]	**C** Q I **P** G **H** A A T G **M**

[a]Ligands of copper are indicated in bold, and proline is marked in red. [b]*Paracoccus denitrificans* (*54*). [c]*Pseudomonas aeruginosa* (*55*). [d]*Alcaligenes faecalis* (*56*). [e]*Populus nigra* (*57*). [f]*Rhus verniciflua* (*58*). [g]*Thiobacillus ferrooxidans* (*59*).

these ET reactions yielded values for the reorganization energy (λ), electronic coupling (H_{AB}), and distance between donor and acceptor that are associated with each of these ET reactions.

The structure of *P. denitrificans* amicyanin exhibits a β-sandwich topology with nine β-strands forming two β-sheets (*20*). The copper center possesses four coordinating ligands when oxidized: two N^{δ} of His52 and His95, S of Cys92, and S of Met98 at a longer distance forming a distorted tetrahedral geometry (Figure 1A). His95, Cys92, and Met98 are located in a "ligand loop" between two β-strands. The crystal structure of the protein complex reveals that both hydrophobic and electrostatic interactions involving several amicyanin residues are important in stabilizing the protein complex (*20*). The hydrophobic patch of amicyanin which interacts with MADH includes residues Met28, Met51, Pro52, Met71, Pro94, Pro96, and Phe97. Arg99 which is at the periphery of this patch is also important as it forms a salt bridge to MADH (Figure 1B). The ligand loops of several type 1 copper proteins (also called cupredoxins) have been structurally characterized (Table 1). The ligand loop is a common feature and believed to contribute to the specificity for associations with redox partner proteins (*21*, *22*). Furthermore, residues in this loop contribute to an array of interactions, including hydrogen-bonding contacts which are thought to be critical for properties of the copper site. The length, sequence, and structure of this loop vary in cupredoxins (*21*). Amicyanin contains the shortest ligand loop and is unusual in that the loop contains two proline residues, Pro94 and Pro96, which are also components of the hydrophobic patch. The presence of a proline between the Cys and His ligands in the ligand loop (Pro94 in *P. denitrificans* amicyanin) is a conserved feature seen in other cupredoxins. However, in the major classes of cupredoxins, a second proline between the His and Met ligands in the loop (Pro96 in *P. denitrificans* amicyanin) is only seen in amicyanin. Furthermore, in *P. denitrificans* amicyanin Pro94 and Pro96 immediately flank the His95 ligand, a structural feature unique among cupredoxins.

The conserved Pro94 was previously altered by site-directed mutagenesis (*23*, *24*), and structural and mechanistic studies of P94F and P94A amicyanins revealed that the E_m value was made more positive due to alteration of H-bonding interactions of copper ligands (*23*). Mutation of another proline present in the hydrophobic patch, Pro52, resulted not only in loss of interactions of the Pro with MADH and but also in repositioning of Met51 which altered the protein−protein interface. This decreased the binding affinity and altered the kinetic mechanism of the ET reaction with MADH (*25*, *26*). To gain more insight into the roles of proline residues of the ligand loop and hydrophobic patch of cupredoxins in their interactions with redox partner proteins and interprotein ET reactions, Pro96 was altered by site-directed mutagenesis, and the consequence on the structure and function of amicyanin was characterized.

EXPERIMENTAL PROCEDURES

Protein Purification. Previously described procedures were used to purify MADH (*27*) and native amicyanin (*5*) from *P. denitrificans*. The protein concentrations were calculated using known extinction coefficients for oxidized amicyanin (ε_{595} = 4610 cm^{-1} M^{-1}) and MADH (ε_{440} = 26200 cm^{-1} M^{-1}). P96A

and P96G amicyanin were expressed in *Escherichia coli* and purified from the periplasmic fraction as described previously for recombinant wild-type amicyanin (*28*). P96G amicyanin was isolated with only partial copper occupancy of the metal site, with some of the site containing zinc instead. The zinc was removed, and the protein was reconstituted with copper as described previously for other amicyanin mutant proteins (*29*, *30*). The extinction coefficients of P96A and P96G amicyanin were determined by anaerobic reductive titration of the fully oxidized protein with a solution of sodium dithionite which had been standardized by titration with native amicyanin.

Site-Directed Mutagenesis of the Amicyanin Gene. Site-directed mutagenesis was performed on double-stranded pMEG201 (*28*), which contains the *mauC* gene which encodes amicyanin, using two mutagenic primers with the QuickChange site-directed mutagenesis kit (Stratagene). The oligonucleotide sequences used to construct the site-directed mutants are as follows: P96A, 5′-TGCACCCCGCATGCCTTCATGCGC-3′ and its cDNA; P96G, 5′-TGCACCCCGCATGGCTTCATGCGC-3′ and its cDNA. The underlined bases are those that were changed to create the desired mutation. The entire 555-base *mauC*-containing fragment was sequenced to ensure that no second site mutations were present, and none were found.

Spectrochemical Redox Potential Determination. The E_m values of P96A and P96G amicyanins were determined by spectrochemical titration as described previously for native amicyanin (*31*). The ambient potential was measured directly with a redox electrode which was calibrated using quinhydrone (a 1:1 mixture of hydroquinone and benzoquinone) as a standard with an E_m value of +286 mV at pH 7.0 (*32*). The reaction mixture contained 130 μM amicyanin in 50 mM BisTris propane buffer at the indicated pH, at 25 °C. The mixture was titrated by addition of incremental amounts ascorbate, which was used as a reductant. In the oxidative direction, titration by addition of potassium ferricyanide was performed. The absorption spectrum of amicyanin was recorded at different potentials (E), and the concentrations of oxidized and reduced amicyanin were determined by comparison with the spectra of the completely oxidized and reduced forms. The E_m was determined from the fit of the data to eq 1.

$$E = E_m + (2.3RT/nF)\log[\text{amicyanin}]_{\text{oxidized}}/[\text{amicyanin}]_{\text{reduced}} \quad (1)$$

For determination of the E_m value of amicyanin in complex with MADH, the reaction mixture contained 20 μM amicyanin and 60 μM MADH in 10 mM potassium phosphate buffer at pH 7.5, at 25 °C. Potassium ferricyaninde (400 μM), quinhydrone (200 μM), and phenanine ethosulfate (20 μM) were present as mediators. The absorption spectrum of the complex was recorded at different potentials, and the concentrations of the oxidized and reduced forms were determined by comparison with the spectra of the completely oxidized complex and a mixture of oxidized MADH with fully reduced amicyanin as described previously (*31*). Data were then analyzed according to eq 1.

Electron Transfer Reactions between MADH and Pro96 Mutant Amicyanins. An Online Instruments (OLIS, Bogard, GA) RSM stopped-flow rapid scanning spectrophotometer was used for the kinetic measurements. Experiments were performed in a 0.01 M potassium phosphate buffer at pH 7.5. The experimental details and methods of data analysis have been previously described (*33*). To study the ET reaction from MADH to amicyanin, prior to mixing one syringe contained reduced (quinol) MADH, and the other contained varying concentrations of oxidized amicyanin. Pseudo-first-order conditions were maintained with excess amicyanin to MADH. ET reactions were fit to the simple kinetic model in eq 2 using eq 3.

$$\text{MADH}_{\text{red}} + \text{amicyanin}_{\text{ox}} \overset{K_d}{\rightleftharpoons} \text{MADH}_{\text{red}} - \text{amicyanin}_{\text{ox}} \overset{k_3}{\underset{k_4}{\rightleftharpoons}} \text{MADH}_{\text{semi}} - \text{amicyanin}_{\text{red}} \quad (2)$$

$$k_{\text{obs}} = k_3[\text{amicyanin}]/([\text{amicyanin}] + K_d) + k_4 \quad (3)$$

Analysis of Electron Transfer Reactions by Electron Transfer Theory. The temperature dependence of k_3 was analyzed according to ET theory (*19*) (eq 4), where H_{AB} is the electronic coupling matrix element, λ is the reorganization energy, h is Plank's constant, T is temperature and R is the gas constant. $\Delta G°$ is determined from the ΔE_m value for the reaction from eq 5, where F is the Faraday constant and n is the number of electrons transferred.

$$k_{ET} = [4\pi^2 H_{AB}{}^2/h(4\pi\lambda RT)^{0.5}]\exp[-(\Delta G°+\lambda)^2/4\lambda RT] \quad (4)$$

$$\Delta G° = -nF\Delta E_m \quad (5)$$

Steady-State Kinetics. Steady-state kinetic experiments were performed as described previously (*34*). For the MADH-catalyzed reduction of amicyanin by methylamine the assay mixtures contained 18 nM MADH and varying concentrations of amicyanin in 0.01 M potassium phosphate buffer at pH 7.5 at 30 °C. Activity was monitored by the change in absorbance caused by the reduction of amicyanin at 595 nm, and the data were fit to eq 6.

$$v/[\text{MADH}] = k_{cat}[\text{amicyanin}]/(K_m + [\text{amicyanin}]) \quad (6)$$

Electron Paramagnetic Resonance (EPR) Spectroscopy. EPR spectra were recorded using a Bruker (Karlsruhe, Germany) X-band spectrometer equipped with an ER 4119HS high-sensitivity cavity at 20 K using an Oxford Instruments low-temperature system. The native and mutant amicyanins were present at a concentration of 300 μM in 10 mM potassium phosphate, pH 7.4, containing 5% glycerol. Each EPR spectrum was recorded under nonsaturating conditions.

Structure Determinations by X-ray Crystallography. P96G amicyanin was dialyzed against 5 mM sodium monobasic/potassium dibasic phosphate buffer, pH 6.6, prior to crystallization trials as was done previously with native and other amicyanin mutants (*30*, *35*). Crystals were grown using the sitting drop method (1.5:1.5 μL protein/reservoir). The protein solution contained ~13 mg/mL protein and 5 mM sodium monobasic/potassium dibasic phosphate buffer, pH 6.6. The reservoir solution contained 1.8 M sodium/potassium phosphate, pH 7.5, including 40 mM ammonium sulfate. The crystal was briefly transferred to fomblin (purchased from Sigma-Aldrich) before freezing in liquid nitrogen and was maintained at 100 K during data collection.

Data sets were measured at a wavelength of 1.140 Å on an ADSC Q315 CCD detector at the 24ID-C beamline equipped with a microdiffractometer MD2 at the NE-CAT, Advance Photon Source. The data were integrated, scaled, and merged using

HKL2000 (*36*). The structure of P96G amicyanin was solved by molecular replacement using the program PHASER (*37*) of PHENIX (*38*). A 1.3 Å resolution crystal structure of the native amicyanin (PDB code 1AAC) with Pro96 mutated to Gly was used as a search model. The resultant model was subjected to refinement using PHENIX (*38*) and a difference Fourier map ($F_o - F_c$) was calculated. The map confirmed the presence of Gly96. The model was subjected to several cycles of alternative positional and thermal parameters, including restrained TLS (translation/libration/screw) refinement as implemented in PHENIX.REFINE (*38*, *39*). The model was corrected and rebuilt wherever necessary using COOT (*40*). For cross-validation (*41*), ~6% (1871 reflections) of all reflections were set aside from refinement for calculation of R_{free}. When the R and R_{free} were 31.2 and 33.7, respectively, water molecules were added to the model. A simulated annealing omit map was calculated around the copper region and Gly96 to remove any model bias. At no point in the refinement were restraints applied to the copper−ligand distances or bond lengths. The simulated annealing refinement was applied once to the model. The final stereochemistry of the model was checked against the Ramachandran map in PROCHECK (*42*). The refined model of P96G amicyanin has four molecules in the asymmetric unit. A summary of the data analysis, refinement results, and stereochemistry is presented in Table 2.

Table 2: Data Collection, Refinement, and Model Statistics for the P96G Amicyanin Structure[a]

	P96G amicyanin
data collection	
wavelength (Å)	1.140
space group	$P3_221$
unit cell dimensions	
a (Å)	97.3
b (Å)	97.3
c (Å)	109.9
resolution limit (Å)	50−2.2
beamline	NE-CAT 24ID-C
$I/\sigma(I)$	23.2 (3.1)
R_{merge} (%)	6.9 (55.7)
completeness (%)	99.8 (100.0)
redundancy	7.2
refinement	
resolution range (Å)	50−2.2
R-factor (%)	23.9
R_{free} (%)	29.1
R-factor (work + test sets) (%)	24.3
no. of reflections	28971
model	
no. of amino acids	420
no. of water molecules	180
no. of copper	4
no. of potassium	1
no. of sodium	2
no. of phosphate	2
average B-factor (Å^2) for protein atoms	49.3
residues in generously allowed regions	2
residues in disallowed regions	0
no. of atoms with zero occupancy	71
stereochemical ideality	
bonds (Å)	0.008
angles (deg)	1.128
dihedral angles (deg)	13.948

[a]Values in parentheses are for the outer shell.

RESULTS

Spectroscopic Properties. The visible absorption spectra of P96A and P96G amicyanin are essentially the same as native amicyanin with an absorption maximum centered at 595 nm (Supporting Information Figure S1 and Table 3). The extinction coefficients of P96A and P96G amicyanin were determined to be 4.6 and 4.9 mM^{-1} cm^{-1}, respectively, as compared to 4.6 mM^{-1} cm^{-1} for native amicyanin. The EPR spectra of oxidized P96A and P96G amicyanins were also nearly identical to that of native amicyanin (Supporting Information Figure S2 and Table 3). For P96A amicyanin the spectra were of the as-isolated protein which has full occupancy of copper. For P96G amicyanin the protein was isolated with zinc present in a large fraction of the protein, and the spectra shown here are of the protein after removal of zinc and reconstitution with copper.

Redox Properties. The redox properties of P96A and P96G amicyanin were determined by spectrochemical titration of each protein, free and in complex with MADH (Table 3). The E_m values of free P96A and P96G amicyanin at pH 7.0 are 9 mV less and 17 mV more positive than native amicyanin, respectively. The E_m value of native amicyanin in complex with MADH is known to decrease on complex formation with MADH because a redox state-dependent conformational change that is linked to the protonation of His95 is sterically constrained in the complex relative to free amicyanin (*31*). This E_m value of amicyanin in complex with MADH is essentially that of free amicyanin in the pH-independent region (> 9.0) and is used for calculation of ΔG° when analyzing ET reactions which occur within the protein complex. The E_m value of P96G amicyanin in complex with MADH was within error of the value in the native complex, and the E_m value of P96A amicyanin in complex with MADH was slightly more positive than in the native complex (Table 3). Thus, these mutations of Pro96 have a minimal effect on the redox properties of amicyanin.

Table 3: Spectroscopic and Redox Properties of Native, P96A, and P96G Amicyanins

	native amicyanin	P96A amicyanin	P96G amicyanin
absorption λ_{max} (nm)	595	595	595
ε_{595} (cm^{-1} mM^{-1})	4.6	4.6	4.9
EPR $g_\perp$	2.06	2.05	2.05
EPR $g_\parallel$	2.24	2.24	2.24
EPR $A_\parallel$ (G)	53	52	51
E_m at pH 7 (free) (mV)	294 ± 7[a]	285 ± 1	311 ± 1
E_m at pH 7 (in complex) (mV)	224 ± 10[a]	241 ± 2	229 ± 3

[a]Taken from ref *31*.

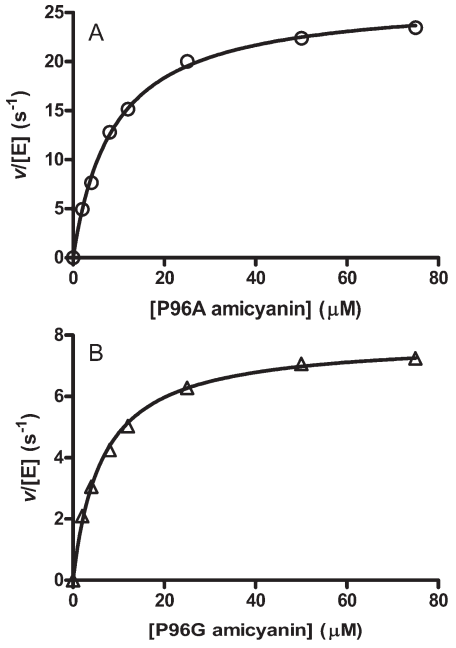

FIGURE 2: Steady-state kinetic analysis of the methylamine-dependent reduction of P96A (A) and P96G (B) amicyanin by MADH. Reaction conditions are described under Experimental Procedures. Lines are fits of the data to eq 6.

Table 4: Steady-State Kinetic Parameters

	native amicyanin[a]	P96A amicyanin	P96G amicyanin
K_m (μM)	1.3 ± 0.3	8.9 ± 0.4	6.4 ± 0.3
k_{cat} (s^{-1})	61 ± 6.0	26.4 ± 0.4	7.9 ± 0.1
k_{cat}/K_m (M^{-1} s^{-1})	4.7×10^7	0.3×10^7	0.1×10^7

[a]Taken from ref *51*.

Steady-State Reactions between MADH and Pro96 Amicyanin Mutants. The steady-state kinetics of methylamine-dependent amicyanin reduction by MADH was examined (Figure 2 and Table 4). P96A and P96G amicyanins exhibited k_{cat} values of 26 and 8 s^{-1}, respectively, compared to 61 s^{-1} for native amicyanin. The K_m value for each mutant was also significantly larger than for native amicyanin. Overall, the P96A and P96G mutations decreased the values of k_{cat}/K_m by 16-fold and 47-fold, respectively.

Electron Transfer Reactions between MADH and Pro96 Amicyanin Mutants. The ET reactions from quinol MADH to P96A and P96G amicyanins were also studied under single-turnover conditions. Values of K_d and k_3 (see eq 2) were obtained from analysis by eq 3 of the dependence on amicyanin concentration of the observed rate of reaction from quinol MADH (Figure 3 and Table 5). The K_d values of P96A and P96G amicyanin were increased approximately 10-fold and 8-fold, respectively. While the $\Delta G°$ values for the ET reactions from quinol MADH to P96A and P96G amicyanin are slightly more favorable than for native amicyanin, the k_3 values for P96A and P96G amicyanins were decreased by 2-fold and 5-fold, respectively. As noted in Table 5, these k_3 and K_d values of P96A and P96G amicyanin are remarkably similar to those previously reported for another mutant, P52G amicyanin (*43*) (discussed later).

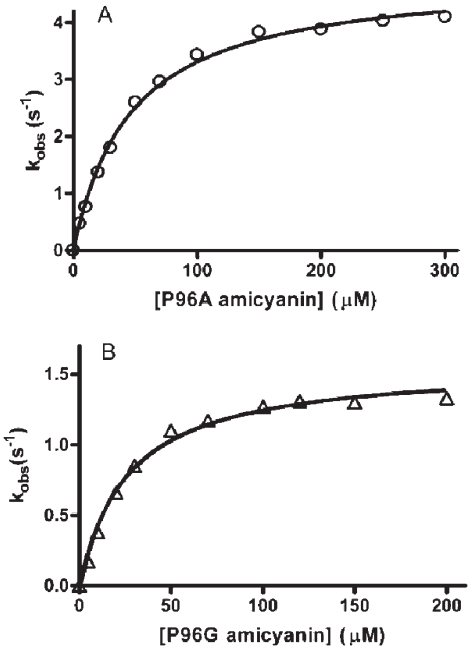

FIGURE 3: Concentration dependence of the observed rate of the ET reaction from MADH to P96A (A) and P96G (B) amicyanin. Reaction conditions are described under Experimental Procedures. Lines are fits of the data to eq 3.

To determine the values of H_{AB} and λ that are associated with these ET reactions, the k_3 values for the ET reaction from quinol MADH to P96A and P96G amicyanins were determined over a range of temperatures, and the data were analyzed using eq 5 (Figure 4). Analysis of these data revealed that the values for both λ and H_{AB} are significantly increased for the reaction with each mutant amicyanin (Table 5). This trend is characteristic of a change in the kinetic mechanism of the redox reaction such that it is no longer a true ET reaction (*44*, *45*). The values of H_{AB} and λ which were obtained were also similar to the parameters that were previously reported for the ET reactions from quinol MADH to P52G amicyanin (Table 5) (*25*). In contrast, the previously reported P94A and P94F amicyanin mutations primarily affected the E_m value, and consequently $\Delta G°$, but did not significantly increase H_{AB} or λ (Table 5) (*23*, *46*).

Crystal Structure of P96G Amicyanin. The structure of oxidized P96G amicyanin was determined at 2.2 Å resolution. P96G amicyanin crystallized in the hexagonal space group $P3_221$, with unit cell parameters $a = b = 97.3$ Å and $c = 109.9$ Å. This space group is different from those of previously crystallized native and mutant amicyanins (*30*, *47*). The refined model of P96G amicyanin has four molecules in the asymmetric unit which together comprise 420 amino acids with 180 water molecules, four coppers, two phosphates, two Na ions, and one K ion. There were 71 atoms (7, 6, 11, and 47 in molecules A, B, C, and D, respectively) which did not have electron density and have been assigned zero occupancy. The average temperature factors (Å^2) for the protein molecules A−D are 64, 46, 60, and 122, respectively, while it is 60 for all of the water molecules. As molecule B exhibited the lowest temperature factor and highest quality of density of the four molecules, subsequent analysis was performed with molecule B.

In general, the structure of P96G amicyanin varies little from that of the native amicyanin. The rms deviation between native (PDB entry 2OV0) and molecule B of P96G amicyanin is 0.62 Å with 103 matched C^α atoms based on the secondary structure

Table 5: Electron Transfer Parameters for the Reactions of Quinol MADH with Native and Mutant Amicyanins

parameter	native amicyanin[a]	P96A amicyanin	P96G amicyanin	P52G amicyanin[b]	P94F amicyanin[c]
K_d (μM)	4.5	47	36	38	< 5
k_3 at 30 °C (s^{-1})	10	5	2	3	60
$\Delta G°$ (kJ mol^{-1})	−3.18	−4.83	−3.47	−4.82	−21.7
λ (eV)	2.3 ± 0.1	2.7 ± 0.1	2.8 ± 0.1	2.8 ± 0.1	2.3 ± 0.1
H_{AB} (cm^{-1})	12 ± 7	42 ± 15	51 ± 14	78 ± 30	4.6 ± 1.3

[a]Taken from ref *14*. [b]Taken from ref *43*. [c]Taken from refs *23* and *46*.

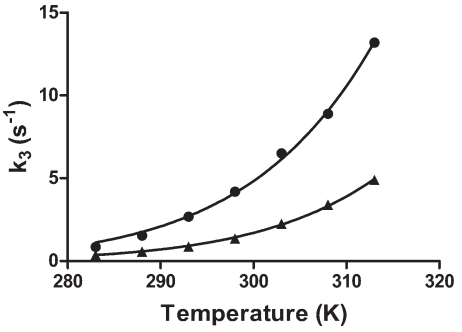

FIGURE 4: Temperature dependence of the observed limiting first-order rate constant for the reactions of reduced MADH with oxidized to P96A (circles) and P96G (triangles) amicyanin. Reaction conditions are described under Experimental Procedures. Lines are fits of the data to eq 4.

matching (*48*) calculated with CCP4MG (*49*) (Figure 5). The difference between native and P96G is most pronounced in the region 15−21. However, it was observed earlier that N-terminal residues 1−21 comprise a very flexible loop segment that adopts variable conformations (*23*). By omitting this segment, the rms deviation drops to 0.29 Å. The mutation caused no significant change in the type 1 copper site, and the copper coordination distances in the P96G amicyanin are very similar to those in native amicyanin (Table 6).

While the overall structure of amicyanin was unchanged as a consequence of the P96G mutation, significant changes were observed in the orientation of residues which have been shown to stabilize the amicyanin−MADH complex. The side chain of Phe97 deviates by ~1 Å. Comparison of the structure of P96G amicyanin with that of native amicyanin in the ternary protein complex reveals that this change in position leads to weakening of the van der Waals interaction between Phe97 and αArg184 of MADH (*28*) (Figure 6). The importance of Phe97 in the interaction with MADH was demonstrated previously as a F97E mutation increased the K_d for complex formation (*28*) and decreased the rate constant for ET from MADH to amicyanin (*50*). The position of the side chain of Arg99 has also changed as a consequence of the P96G mutation such that it is no longer in the proper orientation to form the salt bridge with αAsp167 of MADH that is observed in the structure of the native protein complex (Figure 6). The importance of this ionic interaction toward stabilizing the amicyanin−MADH complex was previously demonstrated by site-directed mutagenesis of Arg99 (*28*) and αAsp167 (*51*). The P96G mutation also eliminates the hydrophobic interactions of Pro96 with MADH.

DISCUSSION

Despite the lack of significant effects of the P96A and P96G mutations on the structure of the type 1 copper site, and spectroscopic

Scheme 1: Kinetic Mechanisms of Electron Transfer Reactions

$$A_{ox}\text{-}B_{red} \underset{k_{-x}}{\overset{k_X}{\rightleftharpoons}} [A_{ox}\text{-}B_{red}]^* \underset{k_{-ET}}{\overset{k_{ET}}{\rightleftharpoons}} A_{red}\text{-}B_{ox}$$

true ET:	$k_{ET} << k_x$	$K_{eq}(k_x/k_{-x}) >> 1$	$k_{obs} = k_{ET}$
gated ET:	$k_X << k_{ET}$		$k_{obs} = k_x$
coupled ET:	$k_{ET} << k_X$	$K_{eq}(k_x/k_{-x}) << 1$	$k_{obs} = K_{eq}* k_{ET}$

and redox properties of amicyanin, these mutations had a significant effect on the rate and mechanism of the ET reaction from MADH, in addition to increasing the K_d for complex formation. The crystal structure of the native MADH−amicyanin complex reveals that Pro96 is present at the protein−protein interface (*8*, *52*). Consistent with that observation, replacement of Pro96 with Ala or Gly increased the K_d values for complex formation 10-fold and 8-fold, respectively. The mutations also caused decreases in the apparent ET rate constant (k_3), which is independent of K_d. Analysis of the temperature dependence of k_3 revealed that the mutations caused significant increases in the experimentally determined values of values H_{AB} and λ. This trend is characteristic of a change in kinetic mechanism from a true ET reaction to one which is either gated or coupled (*45*) (Scheme 1). Gated electron transfer occurs when a relatively slow adiabatic (non electron transfer) reaction precedes and is required to activate the system for a faster nonadiabatic (true electron transfer) reaction. For a gated ET reaction the observed rate constant for the reaction will actually be the rate constant for the preceding slower non-ET reaction step. Coupled electron transfer is a process in which a relatively rapid but thermodynamically unfavorable non electron transfer reaction precedes and is required to activate the system for a relatively slow electron transfer reaction. Since the activated and unreactive states exist in an equilibrium that favors the unreactive state, the observed rate constant (k_{obs}) for the redox reaction is an apparent value equal to the product of the true electron transfer rate constant (k_{ET}) and the equilibrium constant for the preceding non-ET reaction step.

The values for K_d, k_3, H_{AB}, and λ which were determined for the reactions of P96A and P96G amicyanin were very similar to those that were previously reported for the ET reactions from quinol MADH to P52G amicyanin (*43*) (Table 5). A consequence of the P52G amicyanin mutation was also that it altered the position of another residue, Met51. Subsequent study of Met51 amicyanin mutants revealed that the loss of atoms of Pro52 in P52G amicyanin was only responsible for the change in K_d, while the change in position of Met51 in P52G amicyanin was entirely responsible for the change in ET parameters (*26*). Since interactions between the Met51 side chain and MADH were lost as a consequence of the M51A mutation, it was concluded that the mutation slowed the rate of normally rapid conformational

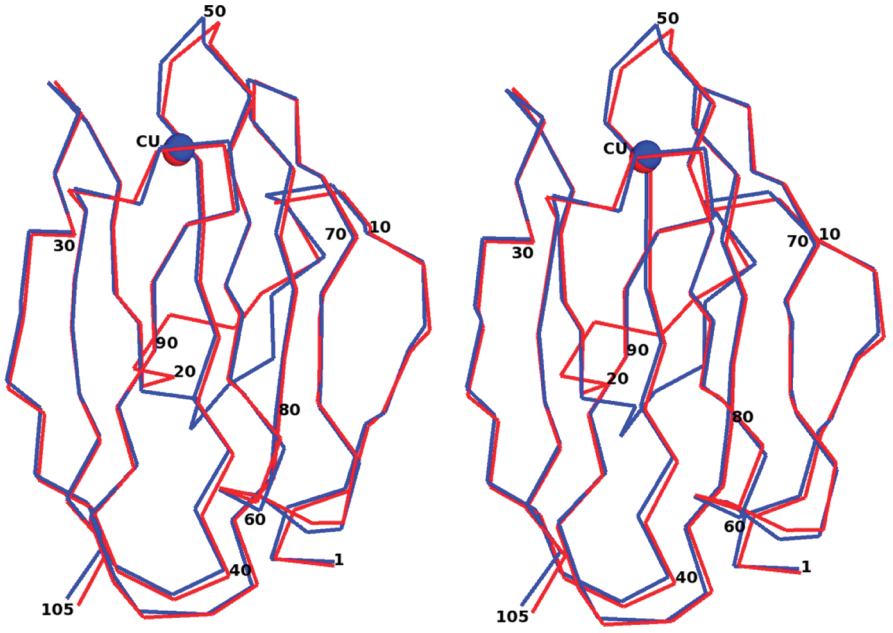

FIGURE 5: Stereoview diagram of the superposition of P96G amicyanin (red) with native amicyanin (blue). The C^{α} trace of protein chains is displayed with residues numbered at a 10-residue interval and copper shown as a blue sphere.

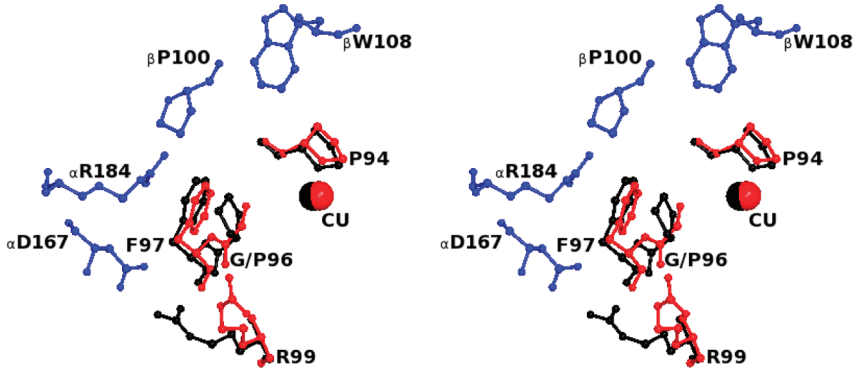

FIGURE 6: Stereview of superposition of P96G amicyanin with native amicyanin within MADH− amicyanin−cytochrome *c*-551i complex (PDB code 2MTA). The α and *β* subunits of MADH are colored blue and shown as ball and stick. Selected residues of P96G amicyanin (red) and native amicyanin (black) are shown as ball and stick with the copper shown as a sphere.

Table 6: Copper Coordination Distances in the Type 1 Sites of P96G and Native Amicyanin

ligand	P96G amicyanin[a]	native amicyanin[b]
Cu−SG/Cys92 (Å)	2.32	2.17
Cu−ND1/His95 (Å)	2.12	2.05
Cu−ND1/His53 (Å)	1.96	1.99
Cu−SD/Met98 (Å)	2.93	3.07

[a]Data for molecule B. [b]Data from PDB entry 2OV0.

rearrangement that precedes ET resulting in conversion of the true ET reaction to a gated ET reaction. These same ET reactions from MADH to native and M51A amicyanin were recently studied using molecular dynamics simulations to estimate the ET coupling strength of ensembles of configurations of the native and mutant protein complex (*53*). It was concluded that hydrophobic residues surrounding the acceptor site on amicyanin comprised a "molecular breakwater" that supports the function of nearby solvent-organizing residues by limiting the exchange of water molecules between the sterically constrained ET region and bulk solvent. It was shown that mutation of Met51 disrupted this breakwater resulting in a decreased availability of the optimum configuration for ET, consistent with the previous experimental results of the effects of this mutation on ET (*26*).

While it may be coincidental, the very similar effects of the Pro96 amicyanin mutations on λ and H_{AB} to those of the P52G and M51A amicyanins suggest that the Pro96 mutations have perturbed the kinetic mechanism for the ET reaction from MADH in a similar manner to that of the P52G mutation. This suggestion is supported by the similar nature of the structural changes that are caused by the respective mutations. As was shown for Pro52, the presence of Pro96 is critical for positioning other residues at the MADH−amicyanin interface. The results indicate that subtle changes in the protein−protein interactions at the MADH−amicyanin interface involving any of multiple residues can cause either a decrease in the relative rate of a configurational rearrangement that is required subsequent to complex formation to poise the system for ET or a decrease in the availability of an optimum configuration for ET from an ensemble of configurations or both. In either case this alters the observed rate constant for the ET reaction as a consequence

of altering the kinetic mechanism of the overall reaction (see Scheme 1). These results highlight the fact that specific individual residues at the surface of redox proteins not only dictate specificity for their redox protein partners but are critical to optimize the configuration of the redox centers and intervening media within the protein complex for the ET event.

The results of these studies also highlight and further define the multiple roles of amino acid residues within the ligand loop of type 1 copper proteins. Previous structural and mechanistic studies of mutations of Pro94, a proline whose presence is conserved in the ligand loops of cupredoxins (Table 1), revealed an important role for this residue in controlling the E_m value of amicyanin. It was shown that mutations of Pro94 to other amino acids resulted in formation of an electron-withdrawing hydrogen bond to the copper-coordinating thiolate sulfur of Cys92 which was introduced by movement of the amide N much closer to the thiolate sulfur than in native amicyanin (*23*). Thus, the conserved proline in this position in the ligand loop is likely required to maintain an appropriate hydrogen-bonding environment for the strong Cys ligand which influences the E_m value. The role of Pro96, a proline whose presence is not conserved in the ligand loops of cupredoxins, is completely different and specifically related to the physiological role of amicyanin. Proline at this position has no effect on the electronic and redox properties of amicyanin. Rather it plays key roles in recognition of its redox partner, as evidenced in alteration of K_d values, and in optimization in the configuration of the redox centers within the complex for ET, as evidenced by alteration of ET parameters diagnostic of a change in the kinetic mechanism of the overall redox reaction. A similar, amicyanin-specific role for a proline was previously identified for Pro52 (*25*). In both the Pro96 and Pro52 mutant amicyanins the effects on the ET reaction mechanism were due to alteration of positions of other residues that interacted with MADH. These results demonstrate how proline residues can significantly affect protein−protein interactions as a consequence of local changes in the structure of the protein backbone which effect the orientations of side chains of nearby amino acid residues. The demonstration of this "indirect" role of proline residues in dictating the specificity of protein−protein interactions is likely not limited to interactions between redox proteins but may be a general feature of specificity of interactions between proteins.

ACKNOWLEDGMENT

We thank M. Elizabeth Graichen and Yu Tang for helpful discussions and technical assistance.

SUPPORTING INFORMATION AVAILABLE

Figures of the absorption and EPR spectra of proteins. This material is available free of charge via the Internet at http://pubs.acs.org.

REFERENCES

1. Gray, H. B. (2003) Biological inorganic chemistry at the beginning of the 21st century. *Proc. Natl. Acad. Sci. U.S.A. 100*, 3563–3568.
2. Adman, E. T. (1991) Copper protein structures. *Adv. Protein Chem. 42*, 145–197.
3. Solomon, E. I., Szilagyi, R. K., DeBeer George, S., and Basumallick, L. (2004) Electronic structures of metal sites in proteins and models: contributions to function in blue copper proteins. *Chem. Rev. 104*, 419–458.
4. Machonkin, T. E., Zhang, H. H., Hedman, B., Hodgson, K. O., and Solomon, E. I. (1998) Spectroscopic and magnetic studies of human ceruloplasmin: identification of a redox-inactive reduced type 1 copper site. *Biochemistry 37*, 9570–9578.
5. Husain, M., and Davidson, V. L. (1985) An inducible periplasmic blue copper protein from *Paracoccus denitrificans*. Purification, properties, and physiological role. *J. Biol. Chem. 260*, 14626–14629.
6. Davidson, V. L. (2001) Pyrroloquinoline quinone (PQQ) from methanol dehydrogenase and tryptophan tryptophylquinone (TTQ) from methylamine dehydrogenase. *Adv. Protein Chem. 58*, 95–140.
7. Husain, M., and Davidson, V. L. (1986) Characterization of two inducible periplasmic *c*-type cytochromes from *Paracoccus denitrificans*. *J. Biol. Chem. 261*, 8577–8580.
8. Chen, L., Durley, R. C., Mathews, F. S., and Davidson, V. L. (1994) Structure of an electron transfer complex: methylamine dehydrogenase, amicyanin, and cytochrome *c*551i. *Science 264*, 86–90.
9. Ferrari, D., Di Valentin, M., Carbonera, D., Merli, A., Chen, Z.-W., Mathews, F. S., Davidson, V. L., and Rossi, G.-L. (2004) Electron transfer in crystals of the binary and ternary complexes of methylamine dehydrogenase with amicyanin and cytochrome *c*551i as detected by EPR spectroscopy. *J. Biol. Inorg. Chem. 9*, 231–237.
10. Ferrari, D., Merli, A., Peracchi, A., Di Valentin, M., Carbonera, D., and Rossi, G. L. (2003) Catalysis and electron transfer in protein crystals: the binary and ternary complexes of methylamine dehydrogenase with electron acceptors. *Biochim. Biophys, Acta 1647*, 337–342.
11. McIntire, W. S., Wemmer, D. E., Chistoserdov, A., and Lidstrom, M. E. (1991) A new cofactor in a prokaryotic enzyme: tryptophan tryptophylquinone as the redox prosthetic group in methylamine dehydrogenase. *Science 252*, 817–824.
12. Davidson, V. L., and Jones, L. H. (1995) Complex formation with methylamine dehydrogenase affects the pathway of electron transfer from amicyanin to cytochrome *c*-551i. *J. Biol. Chem. 270*, 23941–23943.
13. Gray, K. A., Davidson, V. L., and Knaff, D. B. (1988) Complex formation between methylamine dehydrogenase and amicyanin from *Paracoccus denitrificans*. *J. Biol. Chem. 263*, 13987–13990.
14. Brooks, H. B., and Davidson, V. L. (1994) Kinetic and thermodynamic analysis of a physiologic intermolecular electron-transfer reaction between methylamine dehydrogenase and amicyanin. *Biochemistry 33*, 5696–5701.
15. Brooks, H. B., and Davidson, V. L. (1994) Free energy dependence of the electron transfer reaction between methylamine dehydrogenase and amicyanin. *J. Am. Chem. Soc. 116*, 11201–11202.
16. Bishop, G. R., and Davidson, V. L. (1995) Intermolecular electron transfer from substrate-reduced methylamine dehydrogenase to amicyanin is linked to proton transfer. *Biochemistry 34*, 12082–12086.
17. Bishop, G. R., and Davidson, V. L. (1998) Electron transfer from the aminosemiquinone reaction intermediate of methylamine dehydrogenase to amicyanin. *Biochemistry 37*, 11026–11032.
18. Davidson, V. L., and Jones, L. H. (1996) Electron transfer from copper to heme within the methylamine dehydrogenase-amicyanin-cytochrome *c*-551i complex. *Biochemistry 35*, 8120–8125.
19. Marcus, R. A., and Sutin, N. (1985) Electron transfers in chemistry and biology. *Biochim. Biophys. Acta 811*, 265–322.
20. Durley, R., Chen, L., Lim, L. W., Mathews, F. S., and Davidson, V. L. (1993) Crystal structure analysis of amicyanin and apoamicyanin from *Paracoccus denitrificans* at 2.0 Å and 1.8 Å resolution. *Protein Sci. 2*, 739–752.
21. Dennison, C. (2008) The role of ligand-containing loops at copper sites in proteins. *Nat. Prod. Rep. 25*, 15–24.
22. Dennison, C. (2005) Investigating the structure and function of cupredoxins. *Coord. Chem. Rev. 249*, 3025–3054.
23. Carrell, C. J., Sun, D., Jiang, S., Davidson, V. L., and Mathews, F. S. (2004) Structural studies of two mutants of amicyanin from *Paracoccus denitrificans* that stabilize the reduced state of the copper. *Biochemistry 43*, 9372–9380.
24. Sun, D., Li, X., Mathews, F. S., and Davidson, V. L. (2005) Site-directed mutagenesis of proline 94 to alanine in amicyanin converts a true electron transfer reaction into one that is kinetically coupled. *Biochemistry 44*, 7200–7206.
25. Ma, J. K., Carrell, C. J., Mathews, F. S., and Davidson, V. L. (2006) Site-directed mutagenesis of proline 52 to glycine in amicyanin converts a true electron transfer reaction into one that is conformationally gated. *Biochemistry 45*, 8284–8293.
26. Ma, J. K., Wang, Y., Carrell, C. J., Mathews, F. S., and Davidson, V. L. (2007) A single methionine residue dictates the kinetic mechanism of interprotein electron transfer from methylamine dehydrogenase to amicyanin. *Biochemistry 46*, 11137–11146.
27. Davidson, V. L. (1990) Methylamine dehydrogenases from methylotrophic bacteria. *Methods Enzymol. 188*, 241–246.
28. Davidson, V. L., Jones, L. H., Graichen, M. E., Mathews, F. S., and Hosler, J. P. (1997) Factors which stabilize the methylamine dehydrogenase-amicyanin electron transfer protein complex revealed by site-directed mutagenesis. *Biochemistry 36*, 12733–12738.

29. Diederix, R. E., Canters, G. W., and Dennison, C. (2000) The Met99Gln mutant of amicyanin from *Paracoccus versutus*. *Biochemistry 39*, 9551–9560.
30. Choi, M., Sukumar, N., Liu, A., and Davidson, V. L. (2009) Defining the role of the axial ligand of the type 1 copper site in amicyanin by replacement of methionine with leucine. *Biochemistry 48*, 9174–9184.
31. Zhu, Z., Cunane, L. M., Chen, Z., Durley, R. C., Mathews, F. S., and Davidson, V. L. (1998) Molecular basis for interprotein complex-dependent effects on the redox properties of amicyanin. *Biochemistry 37*, 17128–17136.
32. Cammack, R. (1995) in Bioenergetics: A Practical Approach (Brown, G. C., and Cooper, C. E., Eds.) pp 85−109, IRL Press, New York.
33. Bishop, G. R., Brooks, H. B., and Davidson, V. L. (1996) Evidence for a tryptophan tryptophylquinone aminosemiquinone intermediate in the physiologic reaction between methylamine dehydrogenase and amicyanin. *Biochemistry 35*, 8948–8954.
34. Brooks, H. B., Jones, L. H., and Davidson, V. L. (1993) Deuterium kinetic isotope effect and stopped-flow kinetic studies of the quinoprotein methylamine dehydrogenase. *Biochemistry 32*, 2725–2729.
35. Lim, L. W., Mathews, F. S., Husain, M., and Davidson, V. L. (1986) Preliminary X-ray crystallographic study of amicyanin from *Paracoccus denitrificans*. *J. Mol. Biol. 189*, 257–258.
36. Otwinowski, Z., and Minor, W. (1997) Processing of x-ray diffraction data collected by oscillation methods. *Methods Enzymol. 276*, 307–326.
37. McCoy, A. J., Grosse-Kunstleve, R. W., Adams, P. D., Winn, M. D., Storoni, L. C., and Read, R. J. (2007) Phaser crystallographic software. *J. Appl. Crystallogr. 40*, 658–674.
38. Adams, P. D., Grosse-Kunstleve, R. W., Hung, L. W., Ioerger, T. R., McCoy, A. J., Moriarty, N. W., Read, R. J., Sacchettini, J. C., Sauter, N. K., and Terwilliger, T. C. (2002) PHENIX: building new software for automated crystallographic structure determination. *Acta Crystallogr., Sect. D: Biol. Crystallogr. 58*, 1948–1954.
39. Painter, J., and Merritt, E. A. (2006) TLSMD web server for the generation of multi-group TLS models. *J. Appl. Crystallogr. 39*, 109–111.
40. Emsley, P., and Cowtan, K. (2004) Coot: model-building tools for molecular graphics. *Acta Crystallogr., Sect. D: Biol. Crystallogr. 60*, 2126–2132.
41. Brunger, A. T. (1992) Free R value: a novel statistical quantity for assessing the accuracy of crystal structures. *Nature 355*, 472–475.
42. Laskowski, R., Thornton, J., Moss, D., and MacArthur, M. (1993) PROCHECK: a program to check the stereochemical quality of protein structures. *J. Appl. Crystallogr. 26*, 283–291.
43. Ma, J. K., Carrell, C. J., Mathews, F. S., and Davidson, V. L. (2006) Site-directed mutagenesis of proline 52 to glycine in amicyanin converts a true electron transfer reaction into one that is conformationally gated. *Biochemistry 45*, 8284–8293.
44. Davidson, V. L. (2000) What controls the rates of interprotein electron-transfer reactions. *Acc. Chem. Res. 33*, 87–93.
45. Davidson, V. L. (2008) Protein control of true, gated and coupled electron transfer reactions. *Acc. Chem. Res. 41*, 730–738.
46. Sun, D., and Davidson, V. L. (2003) Effects of engineering uphill electron transfer into the methylamine dehydrogenase-amicyanin-cytochrome *c*-551i complex. *Biochemistry 42*, 1772–1776.
47. Cunane, L. M., Chen, Z. W., Durley, R. C., and Mathews, F. S. (1996) X-ray structure of the cupredoxin amicyanin, from *Paracoccus denitrificans*, refined at 1.31 Å resolution. *Acta Crystallogr., Sect. D: Biol. Crystallogr. 52*, 676–686.
48. Krissinel, E., and Henrick, K. (2004) Secondary-structure matching (SSM), a new tool for fast protein structure alignment in three dimensions. *Acta Crystallogr., Sect. D: Biol. Crystallogr. 60*, 2256–2268.
49. Potterton, L., McNicholas, S., Krissinel, E., Gruber, J., Cowtan, K., Emsley, P., Murshudov, G. N., Cohen, S., Perrakis, A., and Noble, M. (2004) Developments in the CCP4 molecular-graphics project. *Acta Crystallogr., Sect. D: Biol. Crystallogr. 60*, 2288–2294.
50. Davidson, V. L., Jones, L. H., and Zhu, Z. (1998) Site-directed mutagenesis of Phe 97 to Glu in amicyanin alters the electronic coupling for interprotein electron transfer from quinol methylamine dehydrogenase. *Biochemistry 37*, 7371–7377.
51. Zhu, Z., Jones, L. H., Graichen, M. E., and Davidson, V. L. (2000) Molecular basis for complex formation between methylamine dehydrogenase and amicyanin revealed by inverse mutagenesis of an interprotein salt bridge. *Biochemistry 39*, 8830–8836.
52. Chen, L., Durley, R., Poliks, B. J., Hamada, K., Chen, Z., Mathews, F. S., Davidson, V. L., Satow, Y., Huizinga, E., and Vellieux, F. M. (1992) Crystal structure of an electron-transfer complex between methylamine dehydrogenase and amicyanin. *Biochemistry 31*, 4959–4964.
53. de la Lande, A., Babcock, N. S., Rezac, J., Sanders, B. C., and Salahub, D. R. (2010) Surface residues dynamically organize water bridges to enhance electron transfer between proteins. *Proc. Natl. Acad. Sci. U.S.A. 107*, 11799–11804.
54. van Spanning, R. J., Wansell, C. W., Reijnders, W. N., Oltmann, L. F., and Stouthamer, A. H. (1990) Mutagenesis of the gene encoding amicyanin of *Paracoccus denitrificans* and the resultant effect on methylamine oxidation. *FEBS Lett. 275*, 217–220.
55. Hoitink, C. W., Woudt, L. P., Turenhout, J. C., van de Kamp, M., and Canters, G. W. (1990) Isolation and sequencing of the *Alcaligenes denitrificans* azurin-encoding gene: comparison with the genes encoding blue copper proteins from *Pseudomonas aeruginosa* and *Alcaligenes faecalis*. *Gene 90*, 15–20.
56. Petratos, K., Banner, D. W., Beppu, T., Wilson, K. S., and Tsernoglou, D. (1987) The crystal structure of pseudoazurin from *Alcaligenes faecalis* S-6 determined at 2.9 Å resolution. *FEBS Lett. 218*, 209–214.
57. Guss, J. M., Bartunik, H. D., and Freeman, H. C. (1992) Accuracy and precision in protein structure analysis: restrained least-squares refinement of the structure of poplar plastocyanin at 1.33 Å resolution. *Acta Crystallogr. B 48*, 790–811.
58. Fields, B. A., Guss, J. M., and Freeman, H. C. (1991) Three-dimensional model for stellacyanin, a "blue" copper-protein. *J. Mol. Biol. 222*, 1053–1065.
59. Nunzi, F., Woudstra, M., Campese, D., Bonicel, J., Morin, D., and Bruschi, M. (1993) Amino-acid sequence of rusticyanin from *Thiobacillus ferrooxidans* and its comparison with other blue copper proteins. *Biochim. Biophys. Acta 1162*, 28–34.